IAA-AAS-DyCoSS2-01-01

GUIDANCE AND CONTROL FOR SPACECRAFT PLANAR RE-PHASING VIA INPUT-SHAPING AND DIFFERENTIAL DRAG

Riccardo Bevilacqua[*] and David Perez[†]

This paper proposes a solution to the problem of re-phasing circular or low eccentricity orbiting, short-distance spacecraft, by integrating existing analytical guidance solutions based on input-shaping and analytical control techniques for differential drag based on Lyapunov theory. The combined guidance and control approach is validated via numerical simulations in a full nonlinear environment using Systems Tool Kit. The results show promise for future onboard implementation on propellant-less spacecraft.

INTRODUCTION

Small spacecraft flying in close proximity for scientific, commercial, and defense applications, are increasingly appealing to space services providers. In fact, for certain applications they are preferable to larger single spacecraft, due to their lower cost, the formations' reconfiguration ability, the possibility of substituting malfunctioning vehicles without aborting the mission, and the inherent redundancy, in general, of a multiple-spacecraft system (Reference 1). However, spacecraft solutions, such as those based on the CubeSat format[‡], present a new set of design challenges, mainly related to the vehicles' limited size and power. The ability to incorporate thrusters and carry on-board propellant is extremely limited on nano-spacecraft weighting a few kilograms (Reference 2). A valid alternative for planar maneuvering of spacecraft relative motion at low Earth orbits (LEO) is represented by atmospheric differential drag, where the differential accelerations necessary to control the satellites are generated by varying the relative cross-wind surface area. C.L. Leonard (Reference 3) introduced this method for generating the control forces that are required by rendezvous maneuvers at LEO (<600 *km*). The differential drag-based methodology allows for virtually propellant-free control of spacecraft relative motion on the orbital plane, since maneuverable dedicated drag surfaces can be powered by solar energy. The differential drag-based methodology was used for the ORBCOMM constellation's formation keeping (Reference 4), and it will be potentially used by the JC2Sat-FF project developed by the Canadian and Japanese Space Agencies (References 5 and 6). It must be noted that differential drag forces only lie in the along-track direction, limiting controllability to the orbital plane. In addition, differential drag forces are usually represented as an on-off control profile (Reference 3). The differential drag concept holds the potential for replacing, or partially substituting, on-board thrusters and

[*] Assistant Professor, Mechanical Aerospace and Nuclear Engineering Department, Rensselaer Polytechnic Institute, 110 8th street, Troy, NY, 12180, USA.
[†] Post-Doctoral Research Associate, Mechanical Aerospace and Nuclear Engineering Department, Rensselaer Polytechnic Institute, 110 8th street, Troy, NY, 12180, USA.
[‡] http://www.cubesat.org/ (retrieved March 6th, 2014)

propellant tanks with clear benefits, especially for long-term, repeated relative maneuvering on the orbital plane. It should be noted that using the differential drag concept results in additional decay on the orbits of the spacecraft whenever their cross-wind surface area is increased.

In order to contribute to the field of spacecraft relative motion control and mission implementation, this paper creates a framework combining analytical guidance solutions for short distance re-phasing, based on along track, on-off control (presented in Reference 7) with an adaptive Lyapunov control method (presented in References 8 and 9). The guidance solutions are based on a technique known as input-shaping, to be described below. Considering that the trajectories can be planned immediately, with no need for numerical iterations, the analytical nature of the solutions supports satellites with limited computing capabilities (e.g.: nano-satellites). The open loop guidance solutions obtained via input-shaping are tracked using a Lyapunov-based control strategy, also analytical and computationally inexpensive, previously developed specifically for differential drag maneuvering (References 8 and 9).

Short distance re-phasing involves baselines up to several kilometers. This is in contrast to cases where the spacecraft may be even on the opposite side of the orbit with respect to the desired final location. The re-phasing maneuvers herein are performed with respect to a (real or virtual) circular reference orbit, with a semi-major axis equal to that of the reference orbit, and in the same orbital plane. In particular, a satellite starting from a circular orbit or a slightly eccentric one, can be re-phased to a new polar angle (if starting from a circular course) or re-phased to have a closed relative motion with respect to a desired point on the reference circular path. In general, the re-phasing solutions proposed in this paper apply to maneuvers going from an equilibrium configuration to a new equilibrium configuration, where equilibrium means a non-drifting state with respect to the final desired target location.

The analytical design of guidance for short distance re-phasing can be valuable not only for a spacecraft's relocation on its orbit but also for spacecraft proximity operations, where the target point can be actually occupied by another space vehicle. In fact, spacecraft rendezvous is an increasingly important topic given the potential for its application, for example, in on-orbit maintenance and servicing missions, spacecraft monitoring, etc. NASA is targeting the development of such missions through its Satellite Servicing Capabilities Office[*]. Additional applications of proximity flight and docking are seen in de-orbiting space debris, another pressing problem for future space exploitation: spacecraft capable of changing their cross-wind surface area may be envisioned docking to inactive resident space objects (RSO), and controlling their decay.

Input-shaping is a convolution technique based on the knowledge of a system's natural frequencies of oscillation. Given a feed-forward control signal, which is designed to perform a desired maneuver but not to take into account potential excitation of undesired oscillations, input-shaping consists of the convolution of the signal itself and a specified train of impulses so that the system's resulting behavior presents minimal residual vibrations at the end of the maneuver. The impulses and their locations in time are computed based on the frequencies that need to be suppressed, i.e., the modes one wants to limit in amplitude. The majority of input-shaping applications fall under the category of flexible structures control, such as space manipulators control, as seen in References 10-17. It is important to emphasize that input-shaping is not intended to reduce the energy of a system, i.e., existing oscillations cannot be damped. However, maneuvers

[*] Brill, J. (March 11, 2012). *About SSCO*. Available: http://ssco.gsfc.nasa.gov/about.html Last accessed March 6th, 2014.

from an equilibrium condition to a new equilibrium are possible. In addition, appropriate modifications of the input-shaping parameters can inject energy into the system, and lead it to a new equilibrium configuration, with desired higher oscillations, as shown in Reference 7. In addition, to differential drag maneuvering, input-shaping can be applied to on-off thrust profiles, maintaining the nature of the control signal.

The main contribution of this paper consists in demonstrating the feasibility of differential drag for rephasing maneuvers, combining an analytical guidance technique (developed in Reference 7) and a control method (developed in References 8 and 9), and simulating their use in a realistic spacecraft relative maneuvering scenario. Thus, illustrating how such analytical approaches could be orchestrated and used in real time, during a real space flight.

SPACECRAFT RELATIVE MOTION DYNAMICS AND INPUT-SHAPING ANALYTICAL GUIDANCE

Spacecraft Relative Motion Dynamics

Spacecraft relative motion dynamics is used to model how a spacecraft moves with respect to the final desired point, regardless of the presence of a reference spacecraft at the re-phasing desired location. Thus, the re-phasing target point can be represented by the origin of a Local Vertical Local Horizontal (LVLH) reference frame, using Hill-Clohessy-Wiltshire (HCW) equations (Reference 18). In such a frame, x points from Earth to the reference spacecraft (virtual or real), y points along the track (direction of motion), and z completes the right-handed frame (see Figure 1). For this paper, the origin of the LVLH frame moves on a circular orbit, with a semi-major axis equal to that of the active spacecraft's orbit.

The out-of-plane (z) and in-plane (xy) motions are usually assumed to be decoupled. In this paper it is assumed that the spacecraft's and its target's re-phasing location lie in the same orbital plane, and the out-of-plane motion will be neglected. Furthermore, it is assumed that the commands to the drag surfaces are on-off, i.e., instantaneously changing from open to close and vice versa (see References 8-9 and 19-22).

The atmospheric differential drag control concept is based on the assumption that two spacecraft can change their respective cross-wind surface area, generating differential values of drag acceleration along track (y), as depicted in Figure 1. In this example, one spacecraft increases its drag by opening a surface, thus lowering its orbit and increasing its speed with respect to the other spacecraft. The main limitations of this propellant-less control are that only planar motion can be addressed (x and y), and that the orbits decay faster whenever the surfaces are opened.

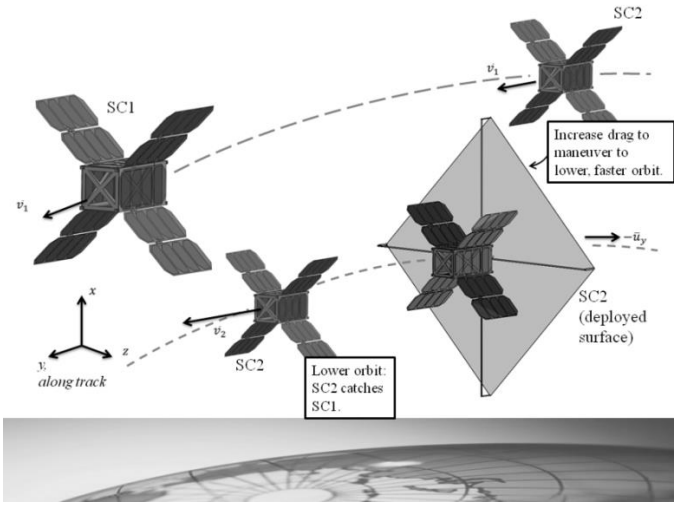

Figure 1. Conceptual sketch explaining differential drag control. Spacecraft 2 increases its drag, thus lowering its orbit and increasing its speed, to catch up with spacecraft 1 in terms of orbital polar angle.

In the equations presented in this paper, bolded symbols represent vectors, while double underlining refers to matrices.

The in-plane, linearized equations of spacecraft relative motion, or HCW equations, described in References 18 and 23, with along-track control only, are given by Equation (1). The assumptions to derive these equations are: two-body force, circular reference orbit, and close proximity.

$$\dot{\boldsymbol{x}} = \boldsymbol{A}\boldsymbol{x} + \boldsymbol{B}u_y, \quad \boldsymbol{A} = \begin{bmatrix} 0 & 0 & 1 & 0 \\ 0 & 0 & 0 & 1 \\ 3\omega^2 & 0 & 0 & 2\omega \\ 0 & 0 & -2\omega & 0 \end{bmatrix}, \boldsymbol{B} = \begin{bmatrix} 0 \\ 0 \\ 0 \\ 1 \end{bmatrix}, \omega = \frac{2\pi}{T} \qquad (1)$$

$$\boldsymbol{x} = \begin{bmatrix} x & y & \dot{x} & \dot{y} \end{bmatrix}$$

where T is the circular orbital period. When drag is used as the control variable, the expression for u_y depends on the atmospheric density, the spacecraft cross-wind surface area, its drag coefficient, mass, and the velocity of the spacecraft relative to the medium. This velocity can be assumed to be equal to the orbital velocity, since the relative velocity between the spacecraft and the origin of the LVLH frame is negligible and the medium can be assumed to rotate with the Earth. As an approximation, the differential is only driven by changes in cross-wind surface area (see References 19 and 20).

Input-shaped control

Input-shaping is based on the concept of providing and then removing energy to/from an oscillatory system. A train of specific impulses, based on the system's natural frequency and damping ratio, are used in convolution with an original control signal, shaping it to achieve the desired final state with minimal residual vibration, as seen in Reference 17.

The train of impulses used herein is defined as a function of the variables y_{fd} (along-track desired final location) and Δt (duration of coasting phases) in Equation (2). The final analytical solution, that takes into account the HCW dynamics and drives the state to the desired final value y_{fd}

is obtained by solving for Δt and an adjusted value of y_{fd}. The control signal to be shaped is chosen as a bang-bang profile of amplitude $\bar{u}$, and a three-impulse shaper as described in Equation (2) (originally presented in Reference 7).

$$
\begin{aligned}
&u_y = A_1 f_{t_1} + A_2 f_{t_2} + A_3 f_{t_3},\ A_1 = \frac{1}{4}, A_2 = \frac{1}{2}, A_3 = \frac{1}{4} \\
&f_{t_1} = \begin{cases} \bar{u}\, sign\left(y_{fd} - y(t_0)\right), & if\ t \le t^*/2 \\ -\bar{u}\, sign\left(y_{fd} - y(t_0)\right), & if\ t^*/2 < t \le t^*, \\ 0, & if\ t > t^* \end{cases} \qquad f_{t_2} = f_{t_1}(t - \Delta t),\ f_{t_3} = f_{t_1}(t - 2\Delta t) \\
&t^* = \sqrt{2\left|y_{fd} - y(t_0)\right| / \bar{u}},
\end{aligned}
\tag{2}
$$

In particular, the quantities A_i in Equation (2) represent the three impulses, convoluted with an original signal. They are given in Reference 15 as $1/(1+K)^2$, $2K/(1+K)^2$, and $K^2/(1+K)^2$, respectively, with $K=exp(-\zeta\pi/(1-\zeta^2)^{1/2})$. ζ indicates the damping ratio of the given dynamic system. The assumed model presents $\zeta=0$, leading to the A_i values in Equation (2).

Control profiles as the one represented in Equation (2) can be tracked using Pulse Width Modulation (PWM) by on-off, single magnitude engines or differential drag devices. Continuously changing profiles are harder to reproduce with PWM. A more effective option is given in previous work using Lyapunov theory to control a nonlinear system with on-off actuation only (see References 8 and 9), as will be shown in the remainder of the paper.

As outlined in Reference 7, the control profile of Equation (2) can be applied on the HCW relative motion equations, obtaining several analytical solutions for rephasing from point to a different point, point to equilibrium relative motion and equilibrium relative motion to another equilibrium relative motion

Analytical solution for leader-follower re-phasing

Re-phasing, in the linear approximation of the LVLH frame means maneuvering the spacecraft from an initial stationary *y* location, to a final, also stationary new *y*. For the remainder of the paper such configurations will be called leader-follower, and so the related re-phasing maneuvers will be named.

In Reference 7, the control signal shown in Equation (2) was applied to the dynamics of Equation (1), starting from an equilibrium leader-follower initial condition ($\boldsymbol{x}(t_0) = [0\ y_0\ 0\ 0]^T$), and considering a variable Δt. This resulted in an analytical expression for the final state, which is not included in this paper for brevity, but can be found in Reference 7. The resulting trajectory will have the center located at the desired along-track location y_{fd}, if a new desired virtual location y_{fd}' (given in Equation (3)) is selected and combined with the expressions for the center of the ellipse representing the final relative orbit ($\bar{x}$ and $\bar{y}$ in Equation (3)).

$$
\begin{aligned}
&y_{fd}' = (2/3)\, y_{fd} + (1/3)\, y_0, \\
&\bar{x} = 4x_f + 2\dot{y}_f/\omega = 0, \bar{y} = y_f - 2\dot{x}_f/\omega = -0.5 y_0 + 1.5 y_{fd}
\end{aligned}
\tag{3}
$$

Using the expression for the final state, Equation (3), and the relative eccentricity (e_{rel}, which represents the physical dimension of the obtained closed orbit), the direct dependency of e_{rel} from Δt was obtained:

$$e_{rel} = 0.5\sqrt{2}\,\frac{\bar{u}}{\omega^2}\sqrt{\begin{aligned}&6\,\mathrm{c}\left(\frac{2}{3}\alpha_2\right) - 4\,\mathrm{c}\left(-\frac{1}{3}\alpha_2 + 2\omega\Delta t\right) - 4\,\mathrm{c}\left(2\omega\Delta t + \frac{1}{3}\alpha_2\right) + c\left(-\frac{2}{3}\alpha_2 + 2\omega\Delta t\right) + \\ &+4\,\mathrm{c}\left(\omega\Delta t - \frac{2}{3}\alpha_2\right) - 16\,\mathrm{c}\left(\frac{1}{3}\alpha_2 + \omega\Delta t\right) - 24\,\mathrm{c}\left(\frac{1}{3}\alpha_2\right) - 16\,\mathrm{c}\left(\omega\Delta t - \frac{1}{3}\alpha_2\right) + \\ &+18 + \mathrm{c}\left(2\omega\Delta t + \frac{2}{3}\alpha_2\right) + 6\,\mathrm{c}\left(2\omega\Delta t\right) + 24\,\mathrm{c}\left(\omega\Delta t\right) + 4\,\mathrm{c}\left(\omega\Delta t + \frac{2}{3}\alpha_2\right)\end{aligned}} \qquad (4)$$

$$\alpha_2 = \omega\sqrt{\frac{3y_{fd} - 3y_0}{\bar{u}}}$$

For a detailed derivation of this expression refer to Reference 7.

If classical input-shaping is applied, with $\Delta t = 0.5T = \pi/\omega$ (Equation (2)), the resulting relative eccentricity is zero, and the final state is obtained as $\boldsymbol{x}(t_f) = [0\ y_{fd}\ 0\ 0]^{\mathrm{T}}$, that is, the initial leader-follower condition (both spacecraft on the same orbit) is reproduced at the end of the maneuver, and the desired along-track baseline is achieved.

Equation (4) also enables the design of different types of re-phasing by adjusting the value of Δt to obtain a final closed relative orbit around the along-track point y_{fd}, with desired relative eccentricity. These types of maneuvers may be envisioned for close approach to a target and "fly-around" for monitoring purposes. In doing this, an oscillation at the end of the maneuver is added, in a quantifiable and desired fashion.

It must be noted that Equation (4) shows 2ω as the highest frequency. The Nyquist–Shannon sampling theorem (see Reference 24) can be used to determine how many points are needed to approximate the function in Equation (4). By computing Equation (4) at Δt points spaced by a $1/(4\omega)$ time distance, that is, theoretically 8π points total (i.e. at least 26) an entire orbital period is approximated. A desired e_{rel} value can be then interpolated using these points (e.g. using splines), posing minimal computational burden. The equilibrium-to-equilibrium e_{rel} case presented later in the paper shows an example of how to set up such approximation and interpolation.

Analytical solution for equilibrium-to-equilibrium closed relative orbit re-phasing

Any maneuver re-phasing an eccentric periodic relative orbit of the active spacecraft with respect to a center point along-track (in the linear LVLH environment) will be called "equilibrium-to-equilibrium". Re-phasing in this case implies shifting the center of this equilibrium relative motion, justifying the choice of the equilibrium-to-equilibrium nomenclature.

The control signal of Equation (2) was applied to on the dynamics of Equation (1), starting from an equilibrium closed relative orbit ($\boldsymbol{x}(t_0) = [x_0\ y_0\ \dot{x}_0\ -2\omega x_0]^T$; Reference 18), and considering a variable Δt, thus yielding an expression for the final state (see Reference 7 for details). The center of the ellipse representing the final relative orbit, computed as in Equation (3), is obtained as

$$\bar{x} = 0,\ \ \bar{y} = y_{fd} - \frac{2}{\omega}\dot{x}_0 \qquad (5)$$

Equation (5) shows that re-phasing to a final equilibrium relative orbit, with center at a desired location, is possible. In fact, starting from t_0, and waiting for any instant when $\dot{x} = 0$ (there are two positions along the closed relative orbit that correspond to this condition), the input-shaped control signal can be applied then. The wait time is given by:

$$t_{wait} = \frac{1}{\omega}\tan^{-1}\left(\frac{\dot{x}_0}{\omega x_0}\right) + k\pi, \qquad k = 0,1,2,... \tag{6}$$

Reference 7 shows how following the same reasoning for the re-phasing from a leader-follower configuration, the direct dependency of e_{rel} from Δt can be obtained as:

$$\Delta e_{rel} = \frac{1}{2}\sqrt{\begin{aligned}&\frac{4}{\omega^4}\left(\begin{aligned}&x_0\omega^2\,\mathrm{c}\left(\frac{2}{3}\alpha_2 + 2\omega\Delta t\right) + \dot{x}_0\omega\,\mathrm{s}\left(\frac{2}{3}\alpha_2 + 2\omega\Delta t\right) + \bar{u}\,\mathrm{s}\left(\frac{2}{3}\alpha_2 + \omega\Delta t\right) + \\ &-\bar{u}\,\mathrm{s}\left(\frac{1}{3}\alpha_2 + 2\omega\Delta t\right) - 2\bar{u}\,\mathrm{s}\left(\frac{1}{3}\alpha_2 + \omega\Delta t\right) + \frac{1}{2}\bar{u}\,\mathrm{s}\left(\frac{2}{3}\alpha_2 + 2\omega\Delta t\right) - \bar{u}\,\mathrm{s}\left(\frac{1}{3}\alpha_2\right) + \\ &+\frac{1}{2}\bar{u}\,\mathrm{s}\left(\frac{2}{3}\alpha_2\right) + \frac{1}{2}\bar{u}\,\mathrm{s}\left(2\omega\Delta t\right) + \bar{u}\,\mathrm{s}\left(\omega\Delta t\right)\end{aligned}\right)^2 + \\ &+\frac{1}{\omega^4}\left(\begin{aligned}&-2x_0\omega^2\,\mathrm{s}\left(\frac{2}{3}\alpha_2 + 2\omega\Delta t\right) + 2\dot{x}_0\omega\,\mathrm{c}\left(\frac{2}{3}\alpha_2 + 2\omega\Delta t\right) - 4\bar{u}\,\mathrm{c}\left(\frac{1}{3}\alpha_2 + \omega\Delta t\right) + \\ &+2\bar{u}\,\mathrm{c}\left(\frac{2}{3}\alpha_2 + \omega\Delta t\right) - 2\bar{u}\,\mathrm{c}\left(\frac{1}{3}\alpha_2 + 2\omega\Delta t\right) + \bar{u}\,\mathrm{c}\left(\frac{2}{3}\alpha_2 + 2\omega\Delta t\right) - 2\bar{u}\,\mathrm{c}\left(\frac{1}{3}\alpha_2\right) + \\ &+\bar{u}\,\mathrm{c}\left(\frac{2}{3}\alpha_2\right) + 2\bar{u}\,\mathrm{c}\left(\omega\Delta t\right) + \bar{u}\,\mathrm{c}\left(2\omega\Delta t\right) + \bar{u}\end{aligned}\right)^2\end{aligned}} \tag{7}$$

$$\alpha_2 = \omega\sqrt{\frac{3y_{fd} - 3y_0}{\bar{u}}}$$

The Nyquist–Shannon sampling theorem (see Reference 24) must be invoked again, to find the number of points to approximate the function in Equation (7), and then interpolation to compute the correct Δt for a desired $\Delta e_{rel.}$.

THE LYAPUNOV-BASED NONLINEAR CONTROLLER FOR DIFFERENTIAL DRAG

The problem of designing a real-time controller using differential drag consists of finding an analytical expression to command the opening or closing of the drag surfaces (see Figure 1) that will force the spacecraft to follow the desired guidance. In particular, the following assumptions are commonly made when using atmospheric differential drag control:

1. The control is only along the *y* direction, as described earlier.
2. The opening/closing of the drag surfaces is instantaneous, i.e., their actuation time is negligible with respect to the duration of the maneuver, resulting in an on-off sequence for commands for opening or closing the drag surfaces.
3. Atmospheric density is known with poor accuracy (~30%, as suggested by previous work (see Reference 19).
4. The drag coefficient can be computed accurately for different geometries, creating a database, using, for example, Direct Simulation Monte-Carlo (see Reference 25).

The poor knowledge of atmospheric density requires the design of robust command logic, capable of dealing with an unknown and continuously variable control magnitude. The authors previously devised such a command strategy, using an adaptive Lyapunov approach. The fine details

of the methodology are presented in References 8 and 9, while only the most important results are presented here, along with a discussion on the expected behavior of the atmospheric density.

The controller is based on the idea of being conservative and maintaining a sufficient margin of control authority on the system. In particular, at the initial time of the maneuver the atmospheric density is underestimated (~30% less than what is provided by atmospheric models, see Reference 26), underestimating the available differential drag. At the same time, the initial adjustable parameters for the controller are chosen such that the initial underestimated differential drag is above a critical, or minimum, value that guarantees Lyapunov stability. From that instant on, the controller's parameters are adapted to maintain a low critical value (shown in Equation (11)). This critical value is the minimum amount of differential drag acceleration that will ensure Lyapunov stability for the controller. This conservative procedure relies on the assumption that in average the atmospheric density will only increase throughout the maneuver, since the orbits of the spacecraft are decaying. The critical differential drag value is maintained low, or possibly reduced throughout the maneuver, by adapting the controller. With this methodology, a positive control margin is maintained between real differential drag and minimum differential drag for Lyapunov stability.

The controller is devised as follows. A quadratic Lyapunov function of the tracking error between the spacecraft state and the desired state (e.g., the input-shaping-designed guidance) is defined as:

$$V_L = \boldsymbol{e}^T \underline{\underline{P}} \boldsymbol{e}, \qquad \boldsymbol{e} = \boldsymbol{x}_n - \boldsymbol{x}, \qquad \underline{\underline{P}} \succ 0 \tag{8}$$

where $\underline{\underline{P}}$ is a symmetric positive definite matrix, $\boldsymbol{e}$ is the tracking error vector, $\boldsymbol{x}_n$ and $\boldsymbol{x}$ are the actual spacecraft relative state vector and a reference desired state vector (the guidance obtained controlling Equation (1) with the input of Equation (2), solved with the solutions in Equations (3) or (5) and (6), depending on the type of maneuver), respectively. The drag surfaces activation strategy is obtained by differentiating Equation (8) with respect to time, and imposing a negative sign in this time derivative, leading to an expression for the $\hat{u}$ signal, indicating the open/closed condition for the drag surfaces (1 = open; 0 = closed; -1 = other S/C opens). See References 8 and 9 for details to obtain the formula in Equation (9)

$$\hat{u} = -sign(\boldsymbol{e}^T \underline{\underline{P}} \boldsymbol{B}) \tag{9}$$

The same steps leading to Equation (9) (see References 8 and 9) define the matrix $\underline{\underline{P}}$ as the solution of the Lyapunov equation

$$\underline{\underline{A}}_d^T \underline{\underline{P}} + \underline{\underline{P}} \underline{\underline{A}}_d = -\underline{\underline{Q}} \tag{10}$$

With $\underline{\underline{Q}}$ a symmetric definite positive matrix and $\underline{\underline{A_d}}$ a Hurwitz matrix. These two matrices are user defined, and represent the controller's adjustable parameters, affecting the Lyapunov function and thus the system's behavior.

The information needed to command the drag surfaces (tracking error and matrix $\underline{\underline{P}}$ and vector $\boldsymbol{B}$ in Equation (9)) would be available in real-time onboard a spacecraft, and the command is a straightforward instruction that poses no issues in terms of onboard computer implementation. In addition, there is no information about the actual density value required by the control law. The Lyapunov algebraic developments also lead to the expression of a critical value (a_{Dcrit}) of differential drag that is needed to maintain stable Lyapunov control (see References 8 and 9 for details). This critical value is given as:

$$a_{Dcrit} = \frac{\boldsymbol{e}^T \underline{\underline{P}} \left(\underline{\underline{A}}_{\boldsymbol{d}} \boldsymbol{x}_n - \boldsymbol{f}\left(\boldsymbol{x}_n\right) + \boldsymbol{B}u_d \right)}{\left| \boldsymbol{e}^T \underline{\underline{P}} \boldsymbol{B} \right|} \tag{11}$$

with $\boldsymbol{f}(\boldsymbol{x}_n)$ representing the nonlinear relative motion dynamics. $\boldsymbol{f}(\boldsymbol{x}_n)$ can be as accurate as the number of higher order gravitational terms that can be expressed analytically. u_d is a desired control, i.e. the acceleration profile generated in the guidance. The analytical expressions for the partial derivatives of the critical value with respect to the adjustable matrices $\underline{\underline{Q}}$ and $\underline{\underline{A}}_{\boldsymbol{d}}$ were developed in References 8 and 9. A real-time adaptation of the matrices themselves (shown in Equation (12)), with the intent to maintain the critical value as low as possible (see References 8 and 9 for details) was designed based on the partial derivatives. In Equation (12) δ_A and δ_Q are increments in the matrices components, chosen such that $\underline{\underline{A}}_d$ remains Hurwitz, and $\underline{\underline{Q}}$ positive definite. The adaptation occurs at discrete time steps, as explained in the simulations section.

$$\begin{aligned} \Delta A_{ij} &= \kappa_A \left[-sign\left(\frac{\partial a_{Dcrit}}{\partial A_{ij}}\right)\delta_A \right], \quad \Delta Q_{ij} = \kappa_Q \left[-sign\left(\frac{\partial a_{Dcrit}}{\partial Q_{ij}}\right)\delta_Q \right] \\ \kappa_A &= \begin{cases} 1 \text{ if } \left|\frac{\partial a_{Dcrit}}{\partial A_{ij}}\right| > \left|\frac{\partial a_{Dcrit}}{\partial A_{kl}}\right| \text{ for } i, j \neq k, l \\ 0 \text{ else} \end{cases}, \kappa_Q = \begin{cases} 1 \text{ if } \left|\frac{\partial a_{Dcrit}}{\partial Q_{ij}}\right| > \left|\frac{\partial a_{Dcrit}}{\partial Q_{kl}}\right| \text{ for } i, j \neq k, l \\ 0 \text{ else} \end{cases} \end{aligned} \tag{12}$$

Depending on the spacecraft computing capabilities the non-adaptive or the adaptive controller can be chosen. The adaptive controller requires the additional computation of the matrix derivative expressions, and the adaptation rule of Equation (12). Once again, all these expressions are analytical, and can be computed provided knowledge of the spacecraft's state vector. Both types of controller perform satisfactorily, as shown in the next section, with expected increased performance when adapting the parameters $\underline{\underline{Q}}$ and $\underline{\underline{A}}_{\boldsymbol{d}}$.

NUMERICAL SIMULATIONS

This section starts by presenting the different types of maneuvers achievable with the analytical guidance, using illustrations obtained from numerical simulations of the linear dynamics, and concludes by illustrating the closed-loop nonlinear simulations and a discussion of the results. In particular, the first subsection shows several leader-follower maneuvers obtained by varying Δt. The second subsection shows the equilibrium-relative-orbit-to-equilibrium-relative-orbit approach, while changing Δt to show how the final relative eccentricity can be varied. The Lyapunov closed-loop control is then used to track the guidance in a full nonlinear environment available in STK. The analytical guidance assumes a maximum control acceleration of approximately 2e-5 m/s^2, typical of atmospheric differential drag at the simulations' given altitude.

It is important to underline that relative navigation is beyond the scope of this paper, and that robust estimation techniques will be needed to accurately compute the analytical guidance and use the closed-loop controller. In the following, perfect knowledge of the relative state between the two spacecraft is assumed, envisioning, for example, a high precision differential GPS technique running on the two spacecraft (example: Reference 27).

Leader-Follower re-phasing guidance

The initial conditions in Table 1, in terms of orbital parameters, are used, with the goal of rephasing the S/C position to match a desired one. The initial location and desired final location are

in the same orbit, with different polar angles. In particular, "backward" and "forward" re-phasing maneuvers are presented.

With the parameters in Table 1 the correct initial S/C state vectors in the LVLH frame centered at the desired target locations are $\boldsymbol{x}(t_0) = 10^3[-0.0013\ -4.2588\ 0\ 0]^T$ for the 27.216 degrees case, and $\boldsymbol{x}(t_0) = 10^3[-0.0009\ 3.5490\ 0\ 0]^T$ for the 27.15 degrees case, with units in meters and meters per second. In the linearized environment, a leader-follower configuration does not present any cross-track displacement nor any along-track velocity component. The linear approximation to obtain the analytical solutions described earlier requires the use of $\boldsymbol{x}(t_0) = 10^3[0\ -4.2588\ 0\ 0]^T$ and $\boldsymbol{x}(t_0) = 10^3[0\ 3.590\ 0\ 0]^T$, respectively .

Table 1. Initial Orbital parameters for S/C and desired location for Leader-Follower case, plus general data for simulations.

Orbital Parameter	Desired	S/C initial
Semi-major axis a	6,778.1 km	6,778.1 km
Eccentricity e	0	0
Inclination i	97.9908 deg	97.9908 deg
Right Ascension of the Ascending Node (*RAAN*) Ω	261.621 deg	261.621 deg
Argument of Perigee ω_p	30 deg	30 deg
Polar Angle υ	27.15 deg and 27.216 deg	27.18 deg

Figure 2 shows the "backwards" maneuver, that is, re-phasing to a smaller polar angle using the input shaping technique of Equation (2). A value of $\Delta t = 0.5T$ is used, corresponding to a new leader-follower configuration.

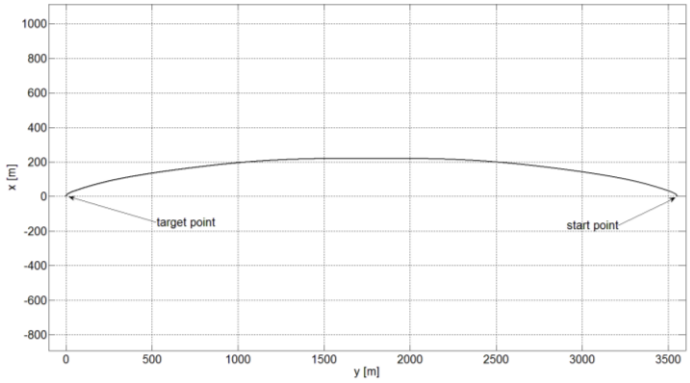

Figure 2. Re-phasing to a lower polar angle, with $\Delta t = 0.5T$, obtaining a new leader-follower configuration (linear dynamics case).

In Figure 3 the "forward" maneuver is shown for three different values of Δt. For $\Delta t = 0.5T$, an input-shaped control is applied, with no residual oscillation at the target point (the LVLH origin). The maximum relative eccentricity is obtained for $\Delta t = 0$, while $\Delta t = 0.25T$ is an example of intermediate relative eccentricity (see Equation (4)) The simulation is propagated beyond the end of the control signal, to show the closed relative motion about the target along-track point.

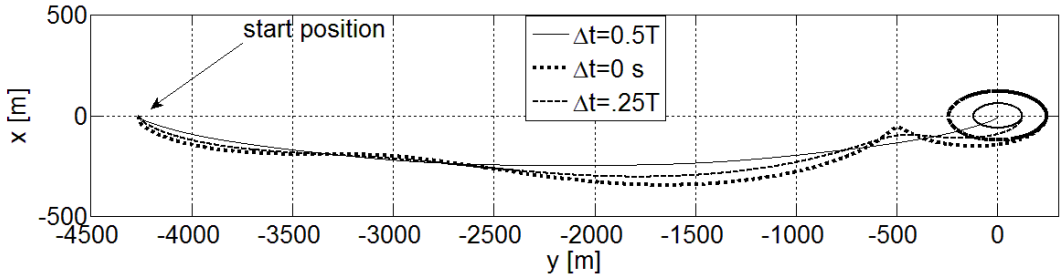

Figure 3. Re-phasing to a higher polar angle. 1) $\Delta t = 0.5T$, obtaining a new leader-follower configuration; 2) $\Delta t = 0$, obtaining the maximum relative eccentricity for the final equilibrium orbit around the target point; 3) $\Delta t = 0.25T$, obtaining an intermediate value of relative eccentricity for the final equilibrium relative orbit around the target point (linear dynamics case).

Equilibrium-relative-orbit-to-equilibrium-relative-orbit re-phasing guidance

The initial conditions in Table 2, in terms of orbital parameters, are used with the goal of re-phasing the S/C, from an equilibrium relative orbit about an initial along-track point, to a final equilibrium relative orbit about a desired final along-track point. In this case, a small eccentricity is given to the S/C, to generate an equilibrium initial relative orbit. The semi-major axes are the same to guarantee bounded-ness of the relative motion. Only a "forward" re-phasing maneuver is presented for this case.

Table 2. Initial Orbital parameters for S/C and desired location for Equilibrium-to-Equilibrium case.

Orbital Parameter	Desired	S/C initial
Semi-major axis a	6,778.1 km	6,778.1 km
Eccentricity e	0	0.0001
Inclination i	97.9908 deg	97.9908 deg
Right Ascension of the Ascending Node (*RAAN*) Ω	261.621 deg	261.621 deg
Argument of Perigee ω_p	30 deg	30 deg
Polar angle υ	27.216 deg	27.18 deg

With the parameters in Table 2 the correct initial S/C state vectors in the LVLH frame, centered at the desired target locations, are $\boldsymbol{x}(t_0) = 10^3[-0.6043\ -4.2584\ 0.0004\ 0.0014]^T$, where the units are m and m/sec. In the linearized environment, an equilibrium configuration requires the modification of this initial condition to $\boldsymbol{x}(t_0) = 10^3[-0.6043\ -4.2584\ 0.0004\ -2\omega x_o]^T$. From the above initial modified condition for the linear model, a waiting time (coasting) is used (Equation (6)), with $k = 0$, before applying the control signal.

Figure 4 represents equilibrium-relative-orbit-to-equilibrium-relative-orbit maneuvers with the same target point as center (origin of LVLH), varying the Δt value. The simulations are propagated beyond the end of the control signal to show the closed relative motion about the target along-track point.

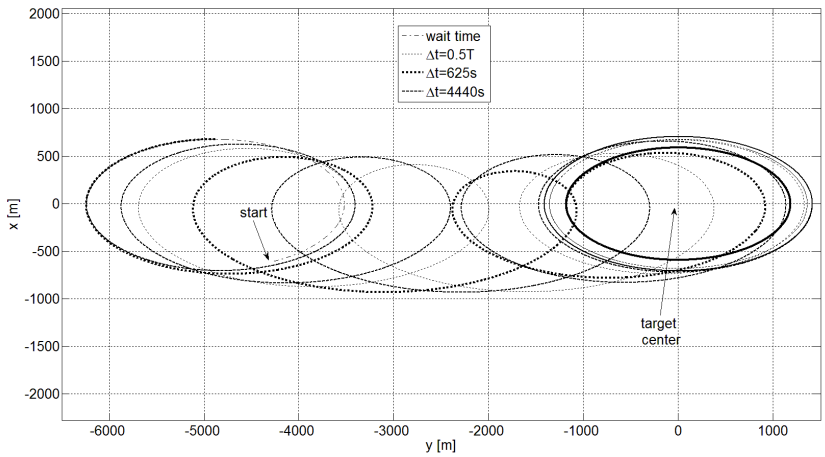

Figure 4. Re-phasing to a higher polar angle for equilibrium-to-equilibrium maneuver. 1) Δt = 0.5T, obtaining an intermediate relative eccentricity (between initial and maximum achievable) on final relative orbit; 2) Δt = 625s, obtaining the minimum relative eccentricity for the final equilibrium orbit around the target point; 3) Δt = 4440s, obtaining the maximum relative eccentricity for the final equilibrium relative orbit around the target point.

The above examples are valid in the simplified linear dynamics case. In order to implement these solutions on a real spacecraft, a closed-loop controller is needed, to track the analytical guidance profiles. This controller is used for the simulations in the following subsection.

Closed-loop control in the full nonlinear case

In this section, the Lyapunov controller described earlier, both the non-adaptive and adaptive versions, is used to track the following guidance:

- **CASE 1**: re-phasing and generation of closed relative orbit at target (Figure 3 with $\Delta t = 0$)
- **CASE 2**: pure re-phasing (Figure 3 with $\Delta t = 0.5T$)
- **CASE 3**: intermediate change of the size of the relative orbit, and re-phasing it (Figure 4 with $\Delta t = 0.5T$)

To reduce the frequency of actuation and allow the drag forces enough time to change the orbits, the controllers are activated every 10 minutes. The same simulations are also run activating the drag devices every 5 minutes to show improvement in accuracy in guidance tracking as the control frequency increases. Numerical simulations are run employing the High Precision Orbital Propagator (HPOP) in Systems Tool Kit (STK) and Matlab. Matlab extracts the relative state vectors from STK, and generates the command to the drag surfaces, going back to STK. An STK scenario with full gravitational field model, variable atmospheric density (using NRLMSISE-00 available in STK) and solar pressure radiation effects is used.

Two identical maneuvering spacecraft are considered, with one at the origin of LVLH, masses of 2kg, maximum surface of 0.5m^2, and minimum of 10cm^2 (representing what is depicted in Figure 1), and standard C_D of 2.2. The initial adaptable matrix $\underline{\underline{A}}_d$ is chosen as $\underline{\underline{A}}$-$\boldsymbol{B}\underline{\underline{K}}$, where $\underline{\underline{A}}$ represents the dynamics matrix of the spacecraft relative motion linear equations, stabilized through a LQR-based $\underline{\underline{K}}$ matrix, to make $\underline{\underline{A}}_d$ Hurwitz. In the LQR problem $\underline{\underline{K}}$ is obtained from $\underline{\underline{Q}}_{LQR} = \underline{\underline{I}}_{4x4}$, and $\underline{\underline{R}}_{LQR}=1.5\cdot10^8$. The initial adaptable matrix $\underline{\underline{Q}}$ is chosen to be $\underline{\underline{I}}_{4x4}\cdot10^{-2}$. The chosen increments for the adaptable matrices in Equation (12) are the values $\delta_A = 10^{-6}$ for $\underline{\underline{A}}_d$ and $\delta_Q = 10^{-6}$ for $\underline{\underline{Q}}$.

The ultimate goals of these simulations are a critical comparison between the two controllers and a discussion helping a potential spacecraft developer in choosing what type of guidance and control should be used on the spacecraft.

CASE 1: Re-phasing from leader-follower, and generating a closed relative motion at the target

Figure 5 shows the results of a nonlinear STK simulation using the Lyapunov controllers to track a re-phasing guidance with final desired closed motion about the target (origin of the LVLH frame) (Figure 3). The simulation is stopped when the guidance reaches its final time. The bottom image clearly shows the benefit of using the adaptive controller versus the non-adaptive. The non-adaptive approach cannot reach the final desired motion, while the adaptation does reach a final motion very close to the desired one. Likewise, the adaptation allows for increased accuracy in tracking the guidance, especially in the last phases of the maneuver, as depicted by the bottom image.

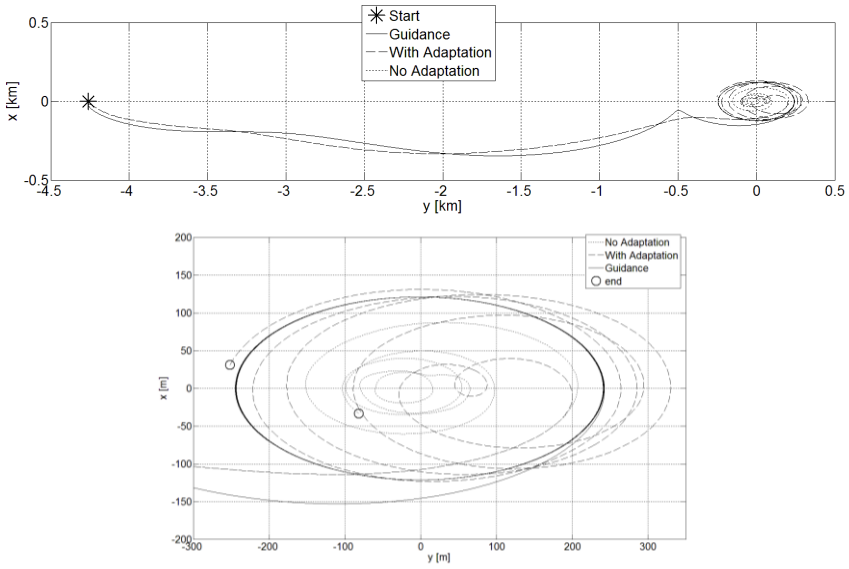

Figure 5. Nonlinear Simulation result (control update every 10 minutes): re-phasing to higher polar angle from leader-follower initial condition and generation of a closed relative motion around the target point. Guidance from Figure 3, with Δt = 0. (TOP) full trajectory; (BOTTOM) zoom of last phase.

Figure 6 shows the same scenario as Figure 5, with an increased control frequency (from 10 to 5 minutes). While an improvement in performance and accuracy is observed for both the adaptive and non-adaptive controllers, the increase in frequency particularly benefits the non-adaptive solution, but it still does not achieve performance equal to that of the adaptive case. This additional result further supports the thesis of preferring adaptation since similar performance can be achieved without the need of increasing frequency of actuation.

CASE 2: re-phasing from leader-follower to leader-follower

Figure 7 shows the results of a nonlinear STK simulation using the Lyapunov controllers to track a pure re-phasing guidance with final desired location at the origin of the LVLH frame (Figure 3). The simulation is stopped when the guidance reaches its final time. As in CASE 1, the bottom image shows that the adaptation allows for better accuracy in tracking the guidance.

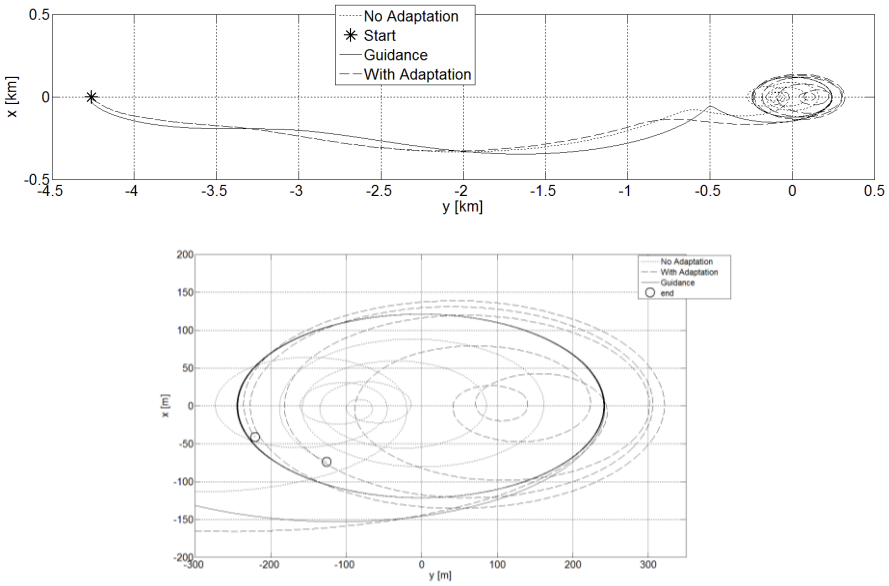

Figure 6. Nonlinear Simulation result (control update every 5 minutes): re-phasing to higher polar angle from leader-follower initial condition and generation of a closed relative motion around the target point. Guidance from Figure 3, with Δt = 0. (TOP) full trajectory; (BOTTOM) zoom of last phase.

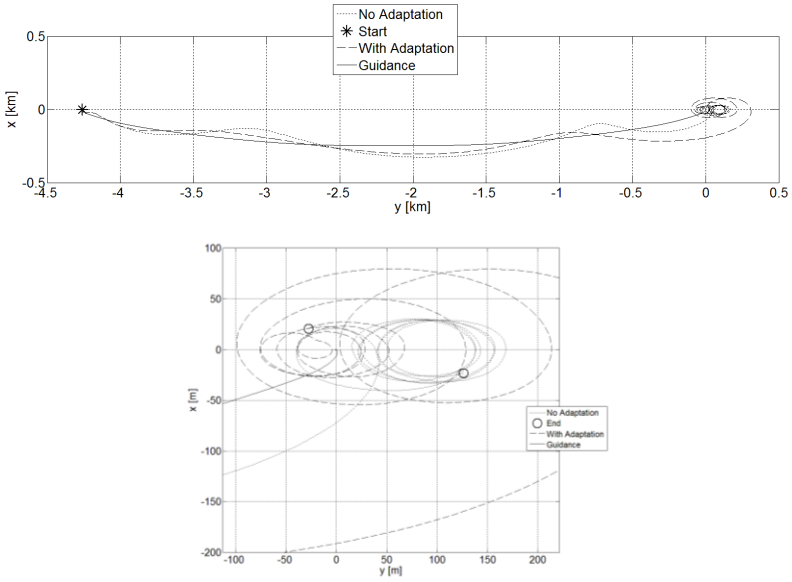

Figure 7. Nonlinear Simulation result (control update every 10 minutes): re-phasing to higher polar angle from leader-follower initial condition to leader-follower final condition. Guidance from Figure 3, with $\Delta t = 0.5T$. (TOP) full trajectory; (BOTTOM) zoom of last phase.

Figure 8 shows the same scenario as Figure 7, with an increased control frequency (from 10 to 5 minutes). In this case both controllers enhance their performance significantly. In particular, the final distance from the desired location reached with the adaptive controller, makes the differential drag approach a viable candidate for very close proximity operations. In fact, such distances are in the order of magnitude of the reach envelope for existing space robotic arms (Canadarm: Reference 28). The maneuver is stopped when the guidance reaches its final time, but additional

control could be performed via differential drag, at a higher frequency of actuation, to move the spacecraft even closer to the target location, or small thrusters could be used for the very final approach for rendezvous and grappling. In addition, as mentioned in the introduction, close distance maneuvering and docking with an inactive spacecraft may enable space debris de-orbiting, due to the deployable surface controlling the drag and thus the decaying orbit.

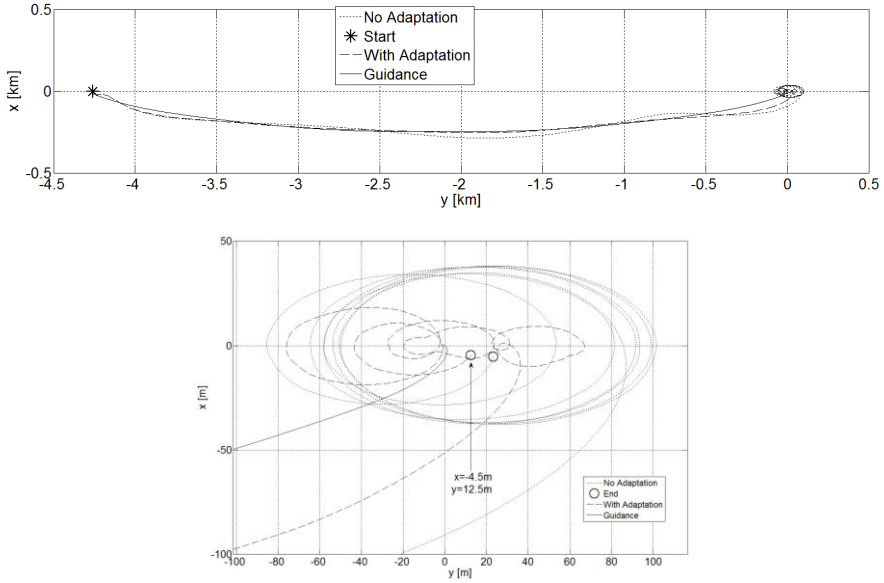

Figure 8. Nonlinear Simulation result (control update every 5 minutes): re-phasing to higher polar angle from leader-follower initial condition to leader-follower final condition. Guidance from Figure 3, with $\Delta t = 0.5T$. (TOP) full trajectory; (BOTTOM) zoom of last phase.

CASE 3: re-phasing from equilibrium-relative-orbit-to-equilibrium-relative-orbit

Figure 9 shows the results of a nonlinear STK simulation using the Lyapunov controllers to track a re-phasing guidance starting from an initial closed relative motion with a final goal of creating a new closed motion around the origin of the LVLH frame (Figure 4). The simulation is stopped when the guidance reaches its final time. The bottom plot shows how the adaptation allows for more precise tracking of the guidance towards the end of the maneuver.

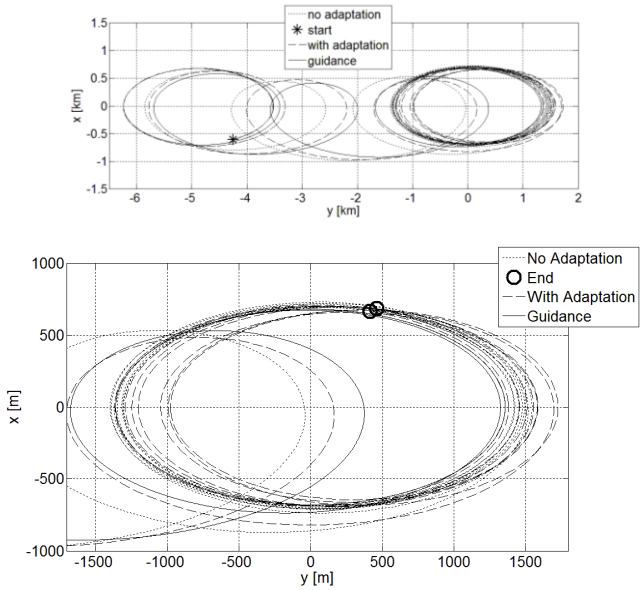

Figure 9. Nonlinear Simulation result (control update every 10 minutes): re-phasing to higher polar angle from equilibrium relative orbit initial condition and generation of a new closed relative motion around the target point. Guidance from Figure 4, with $\Delta t = 0.5T$. (TOP) full trajectory; (BOTTOM) zoom of last phase.

Figure 10 shows the same scenario as Figure 9, with an increased control frequency (from 10 to 5 minutes). In this case in the bottom image it is clear that both controllers provide good tracking. A preliminary interpretation of this behavior can be found in the nature of the maneuver. Since the spacecraft starts with a motion which is already oscillatory, the control action is only required to shift that motion and then stop the shift once the new desired location is reached. Roughly speaking, this maneuver is less challenging from the controller's point of view since the dynamics starts in a favorable initial condition. In CASES 1 and 2 the spacecraft starts in a leader-follower state, thus requiring more effort from the input signal. In CASE 1, the controller is required to move the spacecraft away from its initial state, thus exciting the oscillations as well. These oscillations are controlled by choosing the correct Δt, and there is no need to drive them back to zero. In CASE 2, instead, the controller moves the spacecraft away from its leader-follower state, thus exciting oscillations, but it is also required to drive this motion to zero once the final desired location is approached. Once again, intuitively speaking, this implies more work for the controller. The above described differences in the maneuvers provide an interpretation for the fact that the benefits of adaptation are clearer in CASE 1 and 2 than in CASE 3.

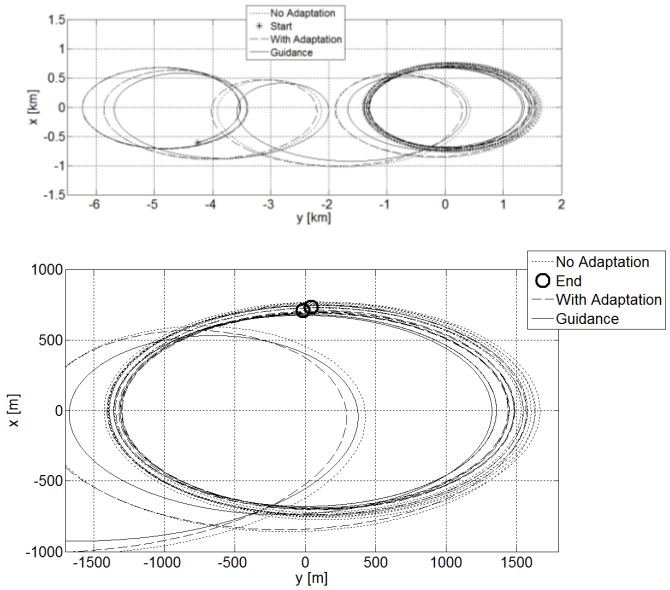

Figure 10. Nonlinear Simulation result (control update every 5 minutes): re-phasing to higher polar angle from equilibrium relative orbit initial condition and generation of a new closed relative motion around the target point. Guidance from Figure 4, with $\Delta t = 0.5T$. (TOP) full trajectory; (BOTTOM) zoom of last phase.

Finally, Table 3 compares adaptive and non-adaptive simulations by showing the number of switches required (i.e. control effort, since electrical power would be required to actuate the devices), the average drag and critical drag, and the average control margin during the maneuvers, where the margin is calculated as the difference between real differential drag (it would not be known in real flight) and critical value. All the values in the table support the preference for the adaptation.

Table 3. Nonlinear simulations results (number of status switches for the drag devices, mean critical and real values of differential drag, and mean differential drag margin).

		10 minutes control update			5 minutes control update		
		Case 1	Case 2	Case 3	Case 1	Case 2	Case 3
	maneuver time (hr)	13.15	16.23	17.55	13.23	16.32	17.63
Non Adaptive	control changes	41	68	64	80	133	127
	mean critical value (m/s^2)	-6.50E-06	-4.30E-06	-3.75E-06	-5.90E-06	-4.51E-06	-3.40E-06
	mean actual drag (m/s^2)	3.38E-05	3.42E-05	3.39E-05	3.37E-05	3.41E-05	3.34E-05
	mean margin(m/s^2)	4.03E-05	3.85E-05	3.77E-05	3.96E-05	3.86E-05	3.68E-05
Adaptive	control changes	37	58	72	76	112	112
	mean critical value (m/s^2)	-7.23E-06	-5.38E-06	-3.81E-06	-6.24E-06	-4.87E-06	-4.28E-06
	mean actual drag (m/sec^2)	3.38E-05	3.44E-05	3.39E-05	3.40E-05	3.41E-05	3.33E-05
	mean margin(m/sec^2)	4.10E-05	3.98E-05	3.77E-05	4.03E-05	3.90E-05	3.75E-05

Results discussion

The examples illustrated in this section lead to the following observations with regards to the performance of the combined guidance and controllers. First of all, both the closed-loop controllers require no numerical iterations, making them viable candidates for onboard implementation. The adaptive controller requires the implementation of the formulas for the derivatives (Reference 8) which is still analytical, but imposes more instructions on the spacecraft computer. Depending on the available memory, the designer may decide to only implement the non-adaptive controller. Overall, the adaptation provides better accuracy and less control effort (number of state switches for the drag surfaces), particularly allowing for better tracking of the guidance as the maneuver approaches the final stages. This is especially true for more demanding maneuvers in terms of guidance, where the dynamics may not be favorable with respect to the final desired state. For cases such as equilibrium-relative-orbit to equilibrium-relative-orbit, the non-adaptive controller may be equivalent to the adaptive in terms of control effort required, that is number of open/closed cycles.

CONCLUSION

This paper introduced a novel framework combining previously presented analytical guidance and Lyapunov control solutions for propellant-less, drag-based spacecraft re-phasing relative maneuvers. The framework studied in this work, provides the groundwork for realistic finite magnitude and finite duration control, such as the control obtained via atmospheric differential drag. The analytical solutions can lead a spacecraft from an initial location along the orbit to a desired final location on the same course, as well as modify its path so that it will fly in an equilibrium fashion about a desired point ahead or behind its initial location. The guidance is graphically illustrated and employed within nonlinear models, where a closed-loop Lyapunov technique is used to track the guidance trajectory with satisfactory accuracy in the full nonlinear STK environment. The relative maneuvers are performed assuming differential drag control capability, which does not use any propellant. Observations derived from the results of the nonlinear simulations provide useful insights to spacecraft developers, and particularly to the mission designer who needs to implement the correct control law on the spacecraft onboard computer.

Overall, the achieved results hold a promise for straightforward implementation onboard real spacecraft, particularly small spacecraft with limited computing capabilities.

ACKNOWLEDGMENTS

The authors wish to acknowledge the United States Air Force Office of Scientific Research (AFOSR) for sponsoring this investigation under the Young Investigator Program (award no. FA9550-12-1-0072).

REFERENCES

[1] Thakker, P., and Shiroma, W., "Emergence of Pico- and Nanosatellites for Atmospheric Research and Technology Testing," *Progress in Astronautics and and Aeronautics, AIAA*, September 15, 2010.

[2] Burges, J. D., Hall, M. J., Lightsey, E. G., "Evaluation of a Dual-Fluid Cold-Gas Thruster Concept", *International Journal of Mechanical and Aerospace Engineering*, 6, 232-237, (2012).

[3] Leonard, C. L., Hollister, W., M., and Bergmann, E. V. "Orbital Formationkeeping with Differential Drag". *AIAA Journal of Guidance, Control and Dynamics,* Vol. 12 (1) (1989), pp.108–113.

[4] Maclay, and C. Tuttle, “Satellite Station-Keeping of the ORBCOMM Constellation Via Active Control of Atmospheric Drag: Operations, Constraints, and Performance,” Advances in the Astronautical Sciences, Vol. 120, Part I, 2005.

[5] De Ruiter, A., Lee, J., Ng, A., “A Fault-tolerant magnetic spin stabilizing controller for the JC2Sat-FF Mission”. *AIAA guidance, navigation and control conference and exhibit*, Honolulu, Hawaii, 18–21 August 2008.

[6] Kumar, B., Ng, A.,Yoshihara, K., De Ruiter, A., “Differential Drag as a Means of Spacecraft Formation Control,” *Proceedings of the 2007 IEEE Aerospace Conference*, Big Sky, MT, March 3-10, 2007.

[7] Bevilacqua, R., “Analytical Guidance Solutions for Spacecraft Planar Re-phasing via Input-Shaping”, *AIAA Journal of Guidance, Control, and Dynamics* (2014). doi: 10.2514/1.G000008

[8] D. Perez, R. Bevilacqua, Differential drag spacecraft rendezvous using an adaptive Lyapunov control strategy, *Acta Astronautica* 83 (2013) 196-207, http://dx.doi.org/10.1016/j.actaastro.2012.09.005

[9] D. Perez, R. Bevilacqua, “Spacecraft Maneuvering via Atmospheric Differential Drag using an Adaptive Lyapunov Controller,” paper AAS 13-440, 23rd AAS/AIAA Spaceflight Mechanics Meeting, Kauai, Hawaii.

[10] A. Banerjee, N. Pedreiro, and W. Singhose, "Vibration Reduction for Flexible Spacecraft Following Momentum Dumping with/without Slewing," *AIAA J. of Guidance, Control, and Dynamics*, vol. 24, pp. 417-428, 2001.

[11] Craig F. Cutforth, Lucy Y. Pao, “Adaptive input shaping for maneuvering flexible structures”, *Automatica*, 40 (2004), 685 – 693. doi:10.1016/j.automatica.2003.11.013

[12] Lucy Y. Pao, “Analysis of the Frequency, Damping, and Total Insensitivities of Input Shaping Designs”, *AIAA Journal of Guidance, Control, and Dynamics*, vol. 20, no. 5, 1997.

[13] Matthew D. Baumgart, Lucy Y. Pao, “Discrete time-optimal command shaping”, *Automatica*, 43 (2007) 1403 – 1409. doi:10.1016/j.automatica.2007.01.003

[14] Mark A. Lau, Lucy Y. Pao, “Input shaping and time-optimal control of flexible structures”, *Automatica*, 39 (2003) 893 – 900. doi:10.1016/S0005-1098(03)00024-4

[15] Lucy Y. Pao, Craig F. Cutforth, “On Frequency-Domain and Time-Domain Input Shaping for Multi-Mode Flexible Structures”, *Journal of Dynamic Systems, Measurement, and Control*, SEPTEMBER 2003, Vol. 125, 494-497. DOI: 10.1115/1.1591808

[16] Lucy Y. Pao, and Mark A. Lau, “Expected Residual Vibration of Traditional and Hybrid Input Shaping Designs”, *AIAA Journal of Guidance, Control, and Dynamics*, Vol. 22, no. 1, 1998, 162-165

[17] M. Romano, B.N. Agrawal, F. Bernelli-Zazzera, "Experiments on Command Shaping Control of a Manipulator with Flexible Links", *AIAA Journal of Guidance, Control, and Dynamics*, Vol. 25, No. 2, 2002, pp. 232-239.

[18] Clohessy, W. H., and Wiltshire, R. S., “Terminal Guidance System for Satellite Rendezvous,” *Journal of Aerospace Sciences*, Vol. 27, No. 9, Sept. 1960, pp. 653–658.

[19] Bevilacqua, R.,Hall, J., S., Romano, M., “Multiple Spacecraft Assembly Maneuvers by Differential Drag and Low Thrust Engines”, *Celestial Mechanics and Dynamical Astronomy* (2010) 106:69–88, DOI 10.1007/s10569-009-9240-3.

[20] Bevilacqua, R., Romano, M., “Rendezvous Maneuvers of Multiple Spacecraft by Differential Drag under J_2 Perturbation”, *AIAA Journal of Guidance, Control and Dynamics*, vol.31 no.6 (1595-1607), 2008. DOI: 10.2514/1.36362

[21] Perez, D., Bevilacqua, R.,"Lyapunov-based Spacecraft Rendezvous Maneuvers using Differential Drag", AIAA-2011-6630 paper, AIAA Guidance, Dynamics and Control Conference 2011, Portland, OR.

[22] Perez, D., Bevilacqua, R., “Differential Drag Spacecraft Rendezvous using an Adaptive Lyapunov Control Strategy”, paper IAA-AAS-DyCoSS1-09-05, 1st International Academy of Astronautics Conference on Dynamics and Control of Space Systems – DyCoSS’2012, Porto, Portugal, 19-21 March 2012.

[23] Hill, G., “Researches in Lunar Theory,” *American Journal of Mathematics*, Vol. 1, No. 1, (1878) 5-26.

[24] C. E. Shannon, "Communication in the presence of noise", *Proc. Institute of Radio Engineers*, vol. 37, no. 1, pp. 10–21, Jan. 1949. Reprint as classic paper in: Proc. IEEE, vol. 86, no. 2, (Feb. 1998)

[25] E. P. Muntz, “Rarefied Gas Dynamics”, Ann. Rev. Fluid Mech. 1989. 21: 387-417.

[26] Bowman, B.R., W.K. Tobiska, F.A. Marcos, C.Y. Huang, C.S. Lin, and W.J. Burke, A New Empirical Thermospheric Density Model JB2008 Using New Solar and Geomagnetic Indices, AIAA/AAS Astrodynamics Specialist Conference, AIAA 2008-6438, 2008

[27] Alfredo Renga, Michele Grassi, Urbano Tancredi, "Carrier-based Differential GPS for autonomous relative navigation in LEO", AIAA Guidance, Navigation, and Control Conference 2012, DOI: 10.2514/6.2012-4707.

[28] Savi Sachdev et al., "CANADA AND THE INTERNATIONAL SPACE STATION PROGRAM: OVERVIEW AND STATUS SINCE IAC 2005", IAC-06-B4.1.3, *57th International Astronautical Congress*, Valencia, Spain, Oct. 2-6, 2006.

[29] Tschauner, J., "The Elliptic Orbit Rendezvous," *4th Aerospace Sciences Meeting*, Los Angeles, CA, 1966. DOI: 10.2514/6.1966-537.